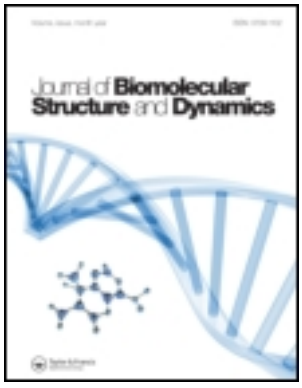

Journal of Biomolecular Structure and Dynamics
Publication details, including instructions for authors and subscription information:
http://www.tandfonline.com/loi/tbsd20

Mechanism of BAG1 repair on Parkinson's disease-linked DJ1 mutation

Calvin Yu-Chian Chen [a b c d]

[a] China Medical University Beigang Hospital, Yunlin, Taiwan

[b] Department of Medical Research, Laboratory of Computational and Systems Biology, China Medical University Hospital, Taichung, 40402, Taiwan

[c] Laboratory of Computational and Systems Biology, China Medical University, Taichung, 40402, Taiwan

[d] Department of Bioinformatics, Asia University, Taichung, 41354, Taiwan

Available online: 09 May 2012

To cite this article: Calvin Yu-Chian Chen (2012): Mechanism of BAG1 repair on Parkinson's disease-linked DJ1 mutation, Journal of Biomolecular Structure and Dynamics, 30:1, 1-12

To link to this article: http://dx.doi.org/10.1080/07391102.2012.674182

Journal of Biomolecular Structure and Dynamics
Vol. 30, No. 1, 2012, 1–12

Taylor & Francis
Taylor & Francis Group

Mechanism of BAG1 repair on Parkinson's disease-linked DJ1 mutation

Calvin Yu-Chian Chen*

China Medical University Beigang Hospital, Yunlin, Taiwan; Department of Medical Research, Laboratory of Computational and Systems Biology, China Medical University Hospital, Taichung 40402, Taiwan; Laboratory of Computational and Systems Biology, China Medical University, Taichung 40402, Taiwan; Department of Bioinformatics, Asia University, Taichung 41354, Taiwan

Communicated by Ramaswamy H. Sarma

(*Received 18 August 2011; final version received 1 January 2012*)

Mutant oncogene DJ1 L166P has been linked to a familial form of early-onset Parkinson's disease (PD). The DJ1 mutant deformed C-terminal helices and prevented the formation of a functional DJ1 dimer. Intriguingly, chaperon modulator, BCL2-associated athanogene (BAG1), has been shown to repair DJ1 mutant and restore its functions. Molecular simulation techniques were employed to elucidate protein–protein interactions between BAG1 and DJ1. Interaction of BAG1 with DJ1 showed recovery of disrupted alpha helix structures and H-bonds stabilizing the functional site Cys106. The His126-Pro184 H-bond (hydrogen-bond) critical to maintaining dimer interfaces was also restored and led to the restoration of dimer formation. High conformational to functional DJ1 dimer was confirmed root mean square deviation = 0.74 Å). Results of this suggest several molecular insights on BAG1–DJ1 repair mechanism and may have an impact on advancing PD treatments.

Keywords: protein–protein interaction; BAG1; molecular dynamics; protein repair; Parkinson's disease

Introduction

Parkinson's disease (PD) is one of the common age-related neurodegenerative disorders in which the etiology remains obscure (Checkoway & Nelson, 1999; de Rijk et al., 2000; Heisters, 2011; Wirdefeldt, Adami, Cole, Trichopoulos, & Mandel, 2011). Nevertheless, a familial form of early-onset PD has been linked to the mutation on *PARK7* gene, which encodes DJ1 protein (Bonifati et al., 2003; Irrcher et al., 2010; Ishikawa et al., 2010; Nuytemans, Theuns, Cruts, & Van Broeckhoven, 2010; Tarantino et al., 2010; Waragai et al., 2007). The major role of DJ1 is to eliminate hydrogen peroxide and hence protect cells from oxidative stress-induced apoptosis (Batelli et al., 2008; Friedman, Xu, & Martin, 2010; Kahle, Waak, & Gasser, 2009; Surmeier et al., 2010; Taira et al., 2004; Ting et al., 2011). DJ1 forms complexes with E3 ubiquitin-protein ligase parkin (PRKN2) and serine/threonine-protein kinase PINK1, which are both PD related proteins, to promote ubiquitination on the neurodegenerative substances (Xiong et al., 2009). Hence, the proteolytic activities of DJ1 have been linked to a neuroprotective function against early onset familial form of PD (Ariga et al., 2011; Hering et al., 2004; Rochet, Liu, Nguyen, Hulleman, & Li, 2008).

Based on analysis of crystal structure, homodimer formation is critical for DJ1 activities (Honbou et al., 2003). The dimer structure favors the proton transfer structure required for protease mechanisms and binding to reactive oxygen species (Honbou et al., 2003; Huai et al., 2003; Wilson, Collins, Hod, Ringe, & Petsko, 2003). In DJ1-linked PD, a mutation on *PARK7* loci resulted in mutant DJ1 L166P has been reported (Miller et al., 2003). The L166P mutation replaced a Leu within a helix seven in the active conformation to a Pro, resulting in severe deformation of helix structures, impairment of DJ1 homodimerization and increased degradation rate (Moore, Zhang, Dawson, & Dawson, 2003; Wilson et al., 2003). This loss-of-function mutation was hypothesized to be a cause to subsequent early-onset of PD and possibly other neurodegenerative diseases (Ariga, Takahashi-Niki, Niki, Taira, & Iguchi-Ariga, 2004; Bekris, Mata, & Zabetian, 2010; Macedo et al., 2003; Mak et al., 2007).

The chaperone HSP70/HSC70 modulator, BCL2-associated athanogene (BAG1), has been reported to

*Email: ycc929@MIT.EDU

ISSN 0739-1102 print/ISSN 1538-0254 online

http://dx.doi.org/10.1080/07391102.2012.674182
http://www.tandfonline.com

restore the function of DJ1 L166P to the dimer conformation (Deeg et al., 2010). BAG1 was originally found to inhibit HSP70/HSC70 chaperone activities (Takayama et al., 1997) and inhibit pro-apoptotic events (Hague et al., 2011; Hung, Roberson, Taft, & Wu, 2003; Kermer et al., 2003, 2009; Sendtner et al., 2005; Townsend, Stephanou, Packham, & Latchman, 2005; Williams et al., 2005). Co-immunoprecipitation has further indicated high binding affinity between DJ1 and BAG1 (Deeg et al., 2010). Nevertheless, the exact DJ1 repair mechanism was not determined.

Recently, computational techniques are commonly employed in computer-aided drug design (Huang et al., 2010), such as screening or predicting potent drugs for specific proteins (Cai, He, & Lu, 2011; Chang, Chen et al., 2011; Chang, Huang, & Chen, 2011a, 2011b; Chang et al., 2010; Chang, Sun et al., 2011; Chang, Wang et al., 2011; Chen, 2010; Chen & Chen, 2010, 2011; Chen, Chang, Chen, & Chen, 2011; Chen, Sun, et al., 2011; Guimaraes, Oliveira, da Cunha, Ramalho, & Franca, 2011; Huang, Lee, Yu, Chen, Hsu et al., 2010; Huang, Lee, Yu, Chen, Tsai et al., 2010; Lin et al., 2011; Mei, Liu, & Yu, 2011; Semighini et al., 2011; Sun, Chang et al., 2011; Sun, Chen, Tsai, Lui, & Chen, 2011; Yang, Chang, & Chen, 2011; Yang, Chang, Chen, & Chen, 2011). In view of the growing reliance on databases as the initial step in drug design, we constructed TCM database@Taiwan (Chen, 2011), a comprehensive TCM small molecule database which currently offers the most extensive catalog of TCM compounds among all available TCM repositories and is organized according to acient traditional Chinese medicine categories as reported in Nature Medicine (Sanderson, 2011). To maximize TCM Database@Taiwan, we have further developed iScreen, the first cloud computing web server for TCM drug screening and *de novo* drug design (Tsai, Chang, & Chen, 2011), and the iSMART (**i**ntegrated **S**yste**M**s Biology **A**ssociated **R**esearch with **T**CM) website to integrate TCM research with computational systems biology resources (Chang, Tsai et al., 2011). Without doubt,

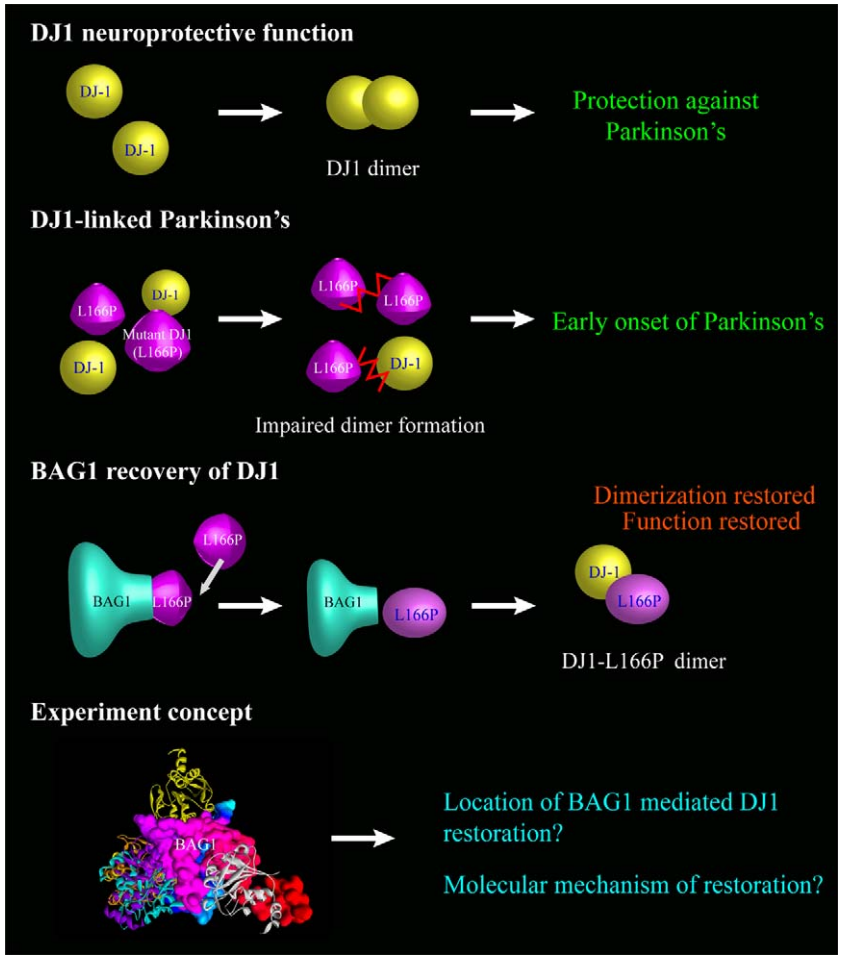

Figure 1. Diagram of experiment concept. DJ1 dimers are required for neuroprotective functions against early onset of familial form of PD. In DJ1-linked PD, L166P mutation causes severe disruption of α helixes. The impaired ability to form dimers is hypothesized to cause early-onset of PD. BAG1 has been demonstrated to restore dimer formation and function of DJ1 L166P. This experiment aims to investigate the location and molecular mechanisms underlying BAG1 mediated restoration of DJ1.

rapid developments in computational hardware and software enable higher efficiency and reliability of virtual screening. In this research, we attempt to provide an explanation on the mechanism of DJ1 function restoration by BAG1 through a computational simulation approach.

Figure 1 illustrates fundamental concepts pertaining to the role of DJ1 in PD, the function of BAG1, and the aim of this study. To test how BAG1 interacts with DJ1 L166P and how the DJ1 functions could be restored, we employed *in silico* simulation to identify potential BAG1–DJ1 mutant interaction interfaces. Considering the lack of complete BAG1 crystal structures, homology modeling was applied. Protein–protein interaction protocol followed by dynamic simulation was expected to provide insights on identifying potential functions of BAG1 in restoring DJ1 functions.

Material and methods

The overall experimental procedure is presented in Figure 2. Specific protocols used within each individual section is detailed in the following sections.

BAG1 homology modeling and validation

DJ1 monomer (protein data bank (PDB): 1PDV) Tao & Tong, 2003 and dimer (PDB: 2R1T) structures were downloaded from RCSB Protein Data Bank. DJ1 L166P mutant model was built and energetically minimized using Build Mutants from Discovery Studio 2.5 (DS 2.5; Accelrys Inc., San Diego, CA), with reference to DJ1 monomer (PDB: 1PDV). BAG1 crystal structures are unavailable, thus the modeled protein structure was built through I-TASSER (http://zhanglab.ccmb.med.umich.edu/I-TASSER/) (Roy, Kucukural, & Zhang, 2010) using the UniProt peptide sequence (ID:Q99933). Predicted structures were compared with known BAG1 partial structures, including the ubiquitin domain (PDB: 1WXV) and BAG domain (PDB: 1HX1) Sondermann et al., 2001, to select the appropriate protein homology model. Validation of the homology model was further verified with Ramachandran and Profile-3D plots.

Protein–protein interaction conformations

Rigid-body docking algorithm, ZDock, was applied for evaluating protein–protein interactions based on the Pairwise Shape Complementarity algorithm (Chen, Li, & Weng, 2003; Chen & Weng, 2003). For DJ1 and BAG1

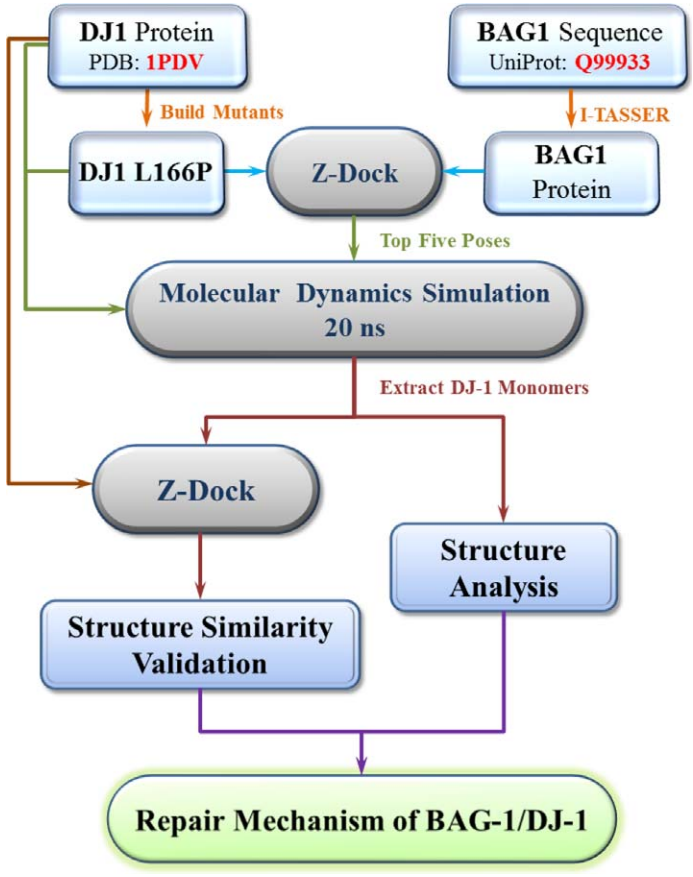

Figure 2. Schematic diagram of experimental design.

interaction, potential docking interfaces were defined by any compatible shapes between the proteins. Angular step size was set at six. Clustering was applied with root mean square deviation (RMSD) cutoff and interface cut-off at 20.0Å.

Molecular dynamics simulation

The following parameters from DS2.5 Simulation Package were applied to each protein–protein interaction conformation for Molecular dynamics (MD) simulation: [solvation model]: explicit periodic boundary; [cell shape]: cubic; and [minimum distance from boundary]: 5 Å. Counter ions of Na^+ and Cl^- were added to neutralize the system. Within each system, a total of 45,400 solvation molecules were added, including 45,160 water molecules, 119 Na^+, and 121 Cl^-. CHARMm force field (Brooks et al., 2009) was applied to the proteins and ions in each MD system. Steepest descent minimization with rigid conformation followed by conjugate gradient minimization with less restrained proteins was applied to each docking pose. Two thousand steps were taken for each minimization step. Each system was then heated to 310 K within 50 ps and then equilibrated at constant temperature for 200 ps. The MD production was applied for 20 ns dynamics simulation based on NVT canonical ensemble (constant temperature). The integration time step was set to 2 fs, and the trajectory snapshots were saved every 20 ps. SHAKE algorithm and Particle Mesh Ewald method were applied to fix hydrogen linked bonds and to treat long-range electrostatics, respectively.

Restoration of DJ1 function and structure

The DJ1 structures from the various DJ1–BAG1 interaction poses were removed after MD and assessed for their ability to form dimers. For clarification purposes, DJ1 monomers removed from different DJ1-BAG1 interaction poses will be named with the pose numbering. The docking interface was based on DJ1 dimer structure (protein data bank (PDB): 2R1T). Angular step size and clustering cut-offs were set at 10.0 Å. Wild-type DJ1, mutant DJ1, or restored DJ1 monomers were docked with a wild-type DJ1 to evaluate the restoration of dimerization ability. Molecular level changes contributing to the recovery of DJ1 function will also be evaluated. Dimers formed by the restored DJ1s were further validated with RMSD using DJ1–DJ1 dimer crystalline structure (PDB: 2R1T) as the reference.

Results and discussion

Validation on BAG1 homology modeling

Five modeled structures of BAG1 were generated by I-TASSER. Each homology model was compared with

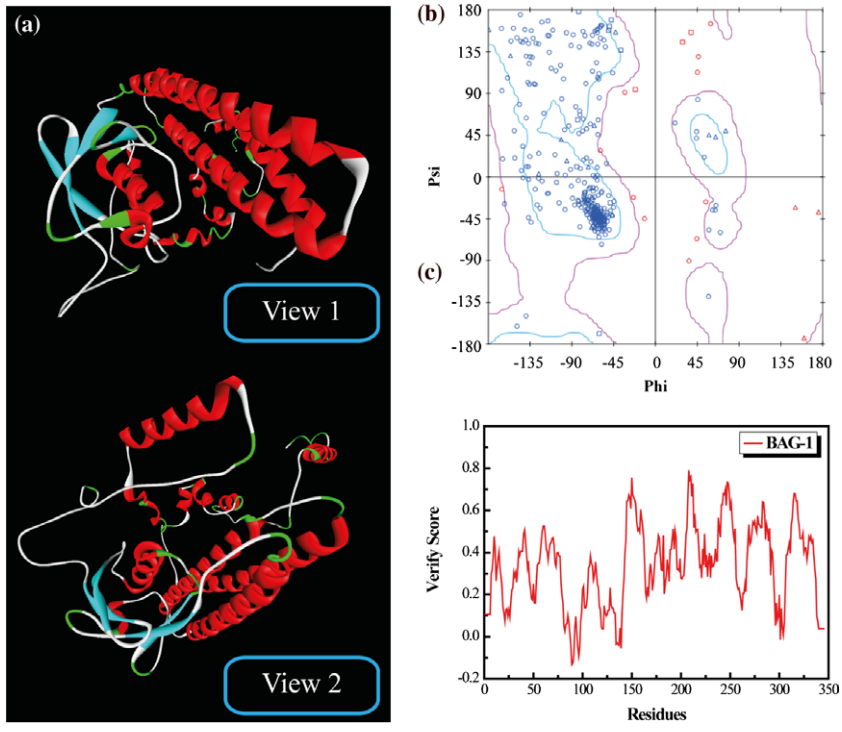

Figure 3. Structure and validation of BAG1 homology model generated by iTasser. (a) Protein structure of top BAG1 homology model generated by iTasser. Alpha helix structures are shown in red, β-sheets in cyan, and turns in green. (b) Ramachandran plot of the generated homology model indicates residue distribution in the allowed, semi-allowed, and disallowed regions is 82, 13, and 5%, respectively. (c) Validation by Profile-3D indicates a reliable model structure.

BAG1 structures of tri-strand β-sheet BAG1 ubiquitin domain (PDB: 1WXV) and tri-helix BAG domain (PDB: 1HX1). The homology model that matched the aforementioned structures is shown in Figure 3(a). As indicated by the Ramachandran plot (Figure 3(b)), 82% residues in the model structure were within the allowed region, 13% in the semi-allowed region, and only 5% residues in the disallowed region. Validity of the modeled structure was further supported by the Profile-3D plot in which majority of the verify scores were greater than zero (Figure 3(c)). Based on these validations, the shown DJ-1 homology model was adopted for this study.

Identification of potential BAG1-DJ1 mutant interaction interfaces

Rigid-body protein–protein interaction simulation via Z-Dock identified five possible binding poses between BAG1 and DJ1. Individual binding poses and the amino acids involved in the interaction interface are shown in Figure 4. Comparison of all docking poses indicated that BAG1 C-terminus tri-helix did not directly interact with DJ1.

Structural recovery by BAG1–DJ1 interaction

A 20 ns MD simulation was conducted to simulate interactions between DJ1 and BAG1 under a dynamic environment. Figure 5 illustrates the RMSD and total energy trajectories of BAG1–DJ1 repair complexes during MD simulation. Regardless of binding pose, the RMSD and total energy trajectories plateaued after 12 ns, indicating stabilization of the complexes. Poses 3 and 4 formed the most stable complexes with BAG1 with total energy levels of approximately −28,000 kcal/mol. Average structures during the final 5 ns of MD were used to investigate structural and molecular level differences in DJ1 induced by BAG1.

Effect of BAG1 on DJ1 monomer structure

The effect of BAG1 on DJ1 monomer structure is summarized in Figure 6. The structure of each monomer at the beginning of MD and the average structure during the final 5 ns of MD are compared to identify structural changes due to MD. No significant differences were observed in wild-type DJ1. In contrast, extensive loss of helicity at α4 and α5 was observed in L166P. In Pose 1, recovery of α4 was observed. However, the extension of Pro109 toward α6 limited the extent of helix recovery in α5. Similar restoration of α4 was also apparent in Pose 2. The restored average structure shows a smooth helix very similar to that of the control DJ1. Restoration of helicity in α5 was initiated as Pro109 rotated toward α4, however, the kink formed by Thr110 and Ala111 remained at the end of MD. Pose 3 showed some restoration of α4, but further helix disruption was seen in α5

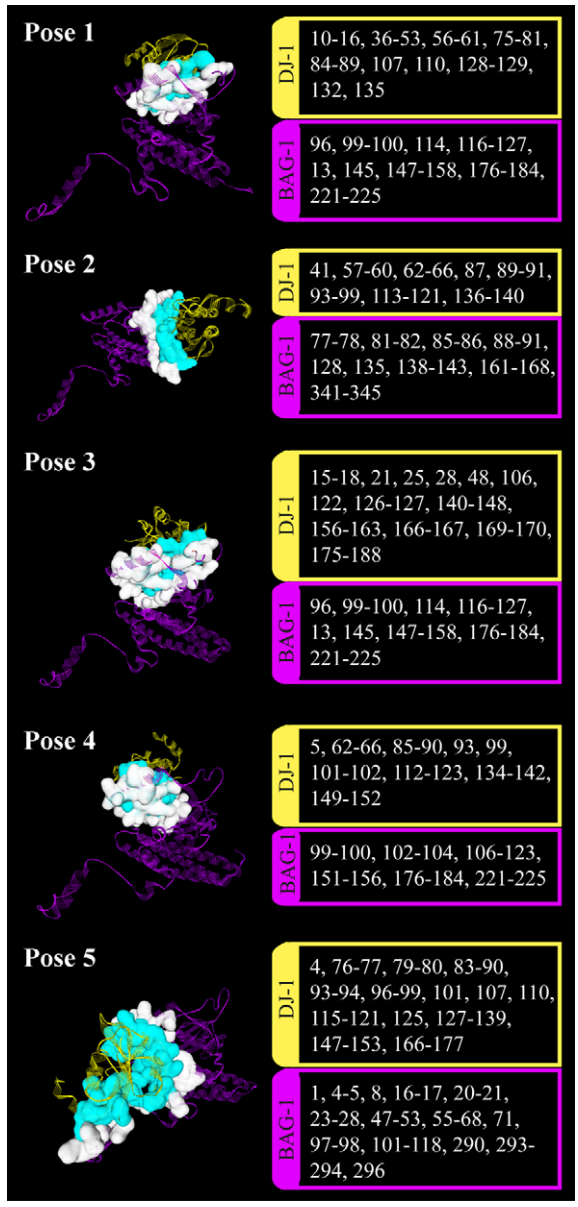

Figure 4. DJ1–BAG1 binding poses generated by ZDock. Violet and yellow ribbons represent BAG1 and DJ1 proteins, respectively. White surfaces represent interaction regions on BAG-1 and cyan surfaces represent interaction regions on DJ1. Interaction residues in each protein are also listed.

and α6. Helix α4 was also recovered in Pose 4, but extensive loss of helicity was apparent in α5 and α6. The average structure of Pose 5 indicated good recovery of α4, α5, and α6. Interaction of mutant DJ1 with BAG1 at Pose 5 resulted in a restored structure that was visually similar to wild type DJ1.

Effect of BAG1 on Cys106 region

The conserved amino acid Cys106 has been proposed to be critical in the reactivity and chaperone functions of

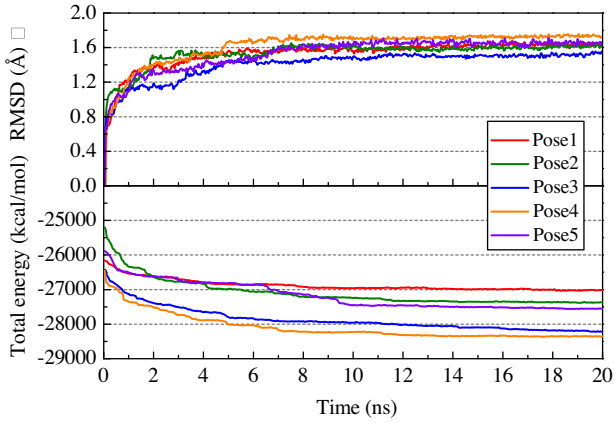

Figure 5. BAG1–DJ1 complex root mean square deviation (RMSD; Å) and total energy trajectories during 20 ns molecular dynamics (MD) simulation.

DJ1 (Anderson & Daggett, 2008; Wilson et al., 2003), thus was naturally of interest to in this investigation. Torsion angle changes related to Cys106 during MD are illustrated in Figure 7. As demonstrated by the small fluctuations in ϕ and ψ angles, Cys106 remained relatively stable throughout the restoration process.

Figure 8 illustrates solvent accessibility and H-bond (hydrogen-bond) network of the Cys106 region. Cys106 remained buried (solvent accessible surface < 10%) in all types of DJ1. This may be important for DJ1 functionality as a delicate balance in the oxidation state of Cys106 must be maintained for appropriate chaperone activities (Anderson & Daggett, 2008; Zhou, Zhu, Wilson, Petsko, & Fink, 2006). In wild-type DJ1, an H-bond was formed between Cys106 and Glu18. This H-bond has been reported to play a major role in dimer formation through its ability to stabilize α1 (Anderson and Daggett, 2008). In addition, His126 is also a key residue for stabilizing opposing DJ1 monomers. Mutant DJ1 that were repaired at Poses 4 and 5 showed restoration of H-bond formation with Glu18 (Figure 8). Poses 2 and 3 did not restore H-bonds with Glu18, but formed H-bond with His126 instead. This is an interesting phenomenon since His126 is involved in forming the critical H-bond (His126-Pro184) in dimers. The H-bond between Cys106 and His126 could bring the functional residue Cys106 closer to the dimer interface and regulating the amount of oxidation that may trigger Cys106 reaction.

Effect of BAG1 on DJ1 dimerization

The ability of DJ-1 to form dimers is critical to its functionality and the key criteria to evaluating the extent of DJ-1 restoration by BAG1. The ability of different recovered DJ-1 to form dimers with wild-type DJ-1 is

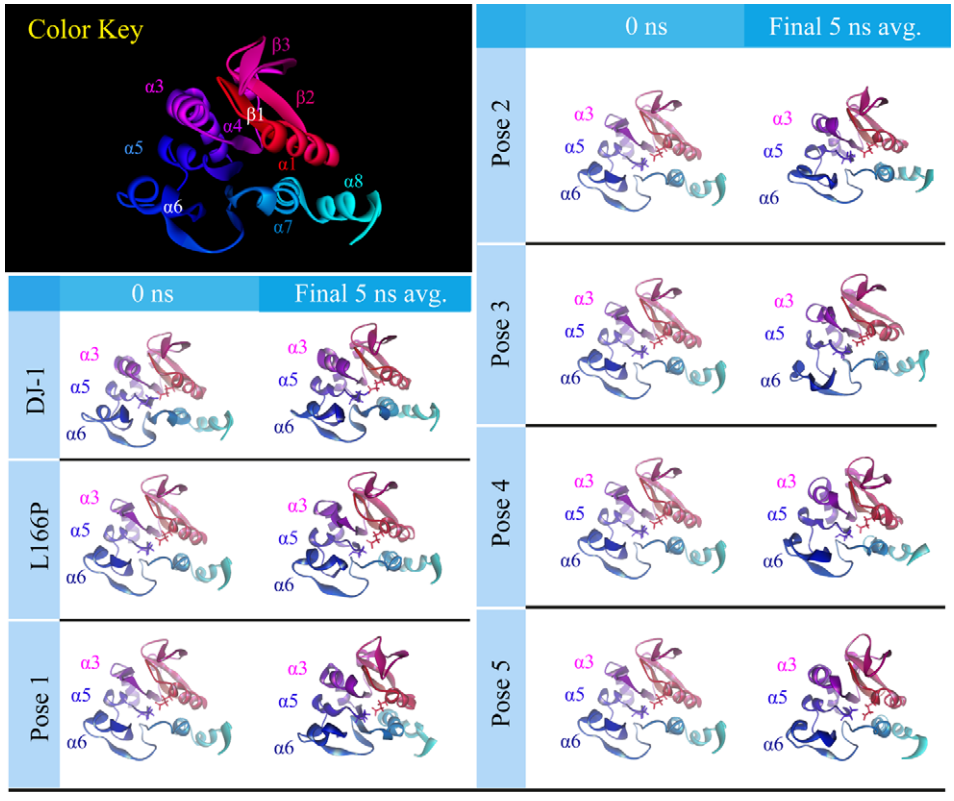

Figure 6. Effect of BAG1 repair on DJ1 monomer structure. Protein conformation at 0 ns and the average structure of the final 5 ns of MD are shown for each type of DJ1.

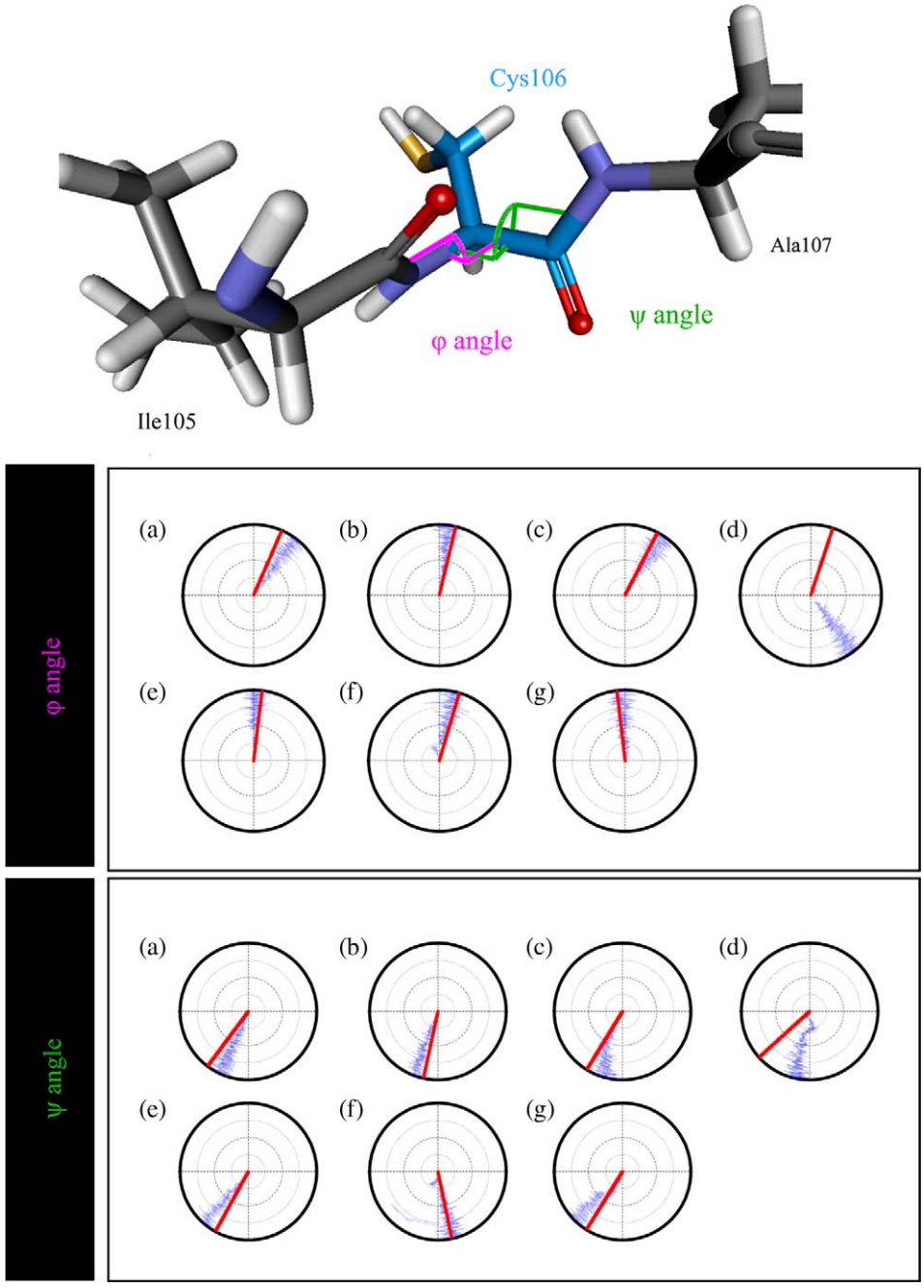

Figure 7. Torsion angle changes in DJ1 Cys106 during 20 ns MD. Torsion angles shown include (a) wild-type DJ1, (b) L166P, (c) Pose 1, (d) Pose 2, (e) Pose 3, (f) Pose 4, and (g) Pose 5.

illustrated in Figure 9. Under the dimerization protocol given, Pose 3 and Pose 4 could not form dimers with wild-type DJ-1. The dimerization of Poses 1, 2, and 5 with wild-type DJ-1 are shown in Figure 9. Based on the DJ1 dimer (PDB: 2R1T) structure, α-helices α1 (Glu15-Gly30) and α7 (Pro158-Asn176) are important structures directly involved in dimer formation. In addition, the H-bond formed between His126 and Pro184 of opposing monomers is critical for stabilizing the dimer interface. We deemed that these structures should be maintained or restored for proper dimerization. Figure 10 illustrates the different helix conformations and H-bonds formed at the dimer interface. In the DJ1–DJ1 dimer, helix structures and the integrity of their spatial arrangements are maintained by the His126-Pro184 H-bonds on either side of the dimer interface. When wild-type DJ1 is substituted

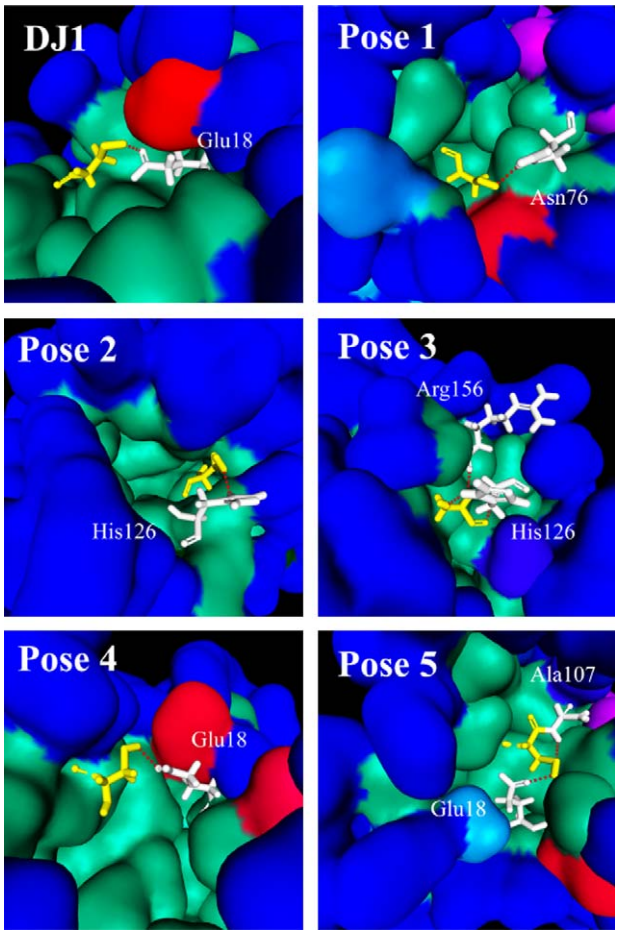

Figure 8. H-bond network formed by Cys106 in DJ1. Protein coloring is based on the solvent accessibility of the respective protein residue. Residues exceeding 25% solvent accessible surface (SAS) is designated as exposed (blue). Residues with less than 10% SAS are designated as buried (green). Cys106 is shown in yellow, and H-bonds formed by Cys106 are illustrated in red.

with the mutant DJ1 L166P, the distance between His126 and Pro184 increases to more than 4 Å. Without the anchoring H-bond, the interface is easily disrupted, hindering the formation of a stable dimer. These structural changes in DJ1 L166P are consistent with previous research (Anderson and Daggett, 2008). Pose 1 DJ1 exhibited similar interface characteristics to L166P. The H-bond distances at both ends of the interface measured 4.23 and 3.99 Å, respectively. In Pose 2 and Pose 5, instability of the critical H-bonds was restored. The H-bond distance between His126 and Pro184 averaged 2.77 Å in Pose 2 and 2.82 in Pose 5.

Validation of restored mutant DJ1 structure

Whilst formation of the critical H-bond between His126 and Pro184 did not differ much between Pose 2 and Pose

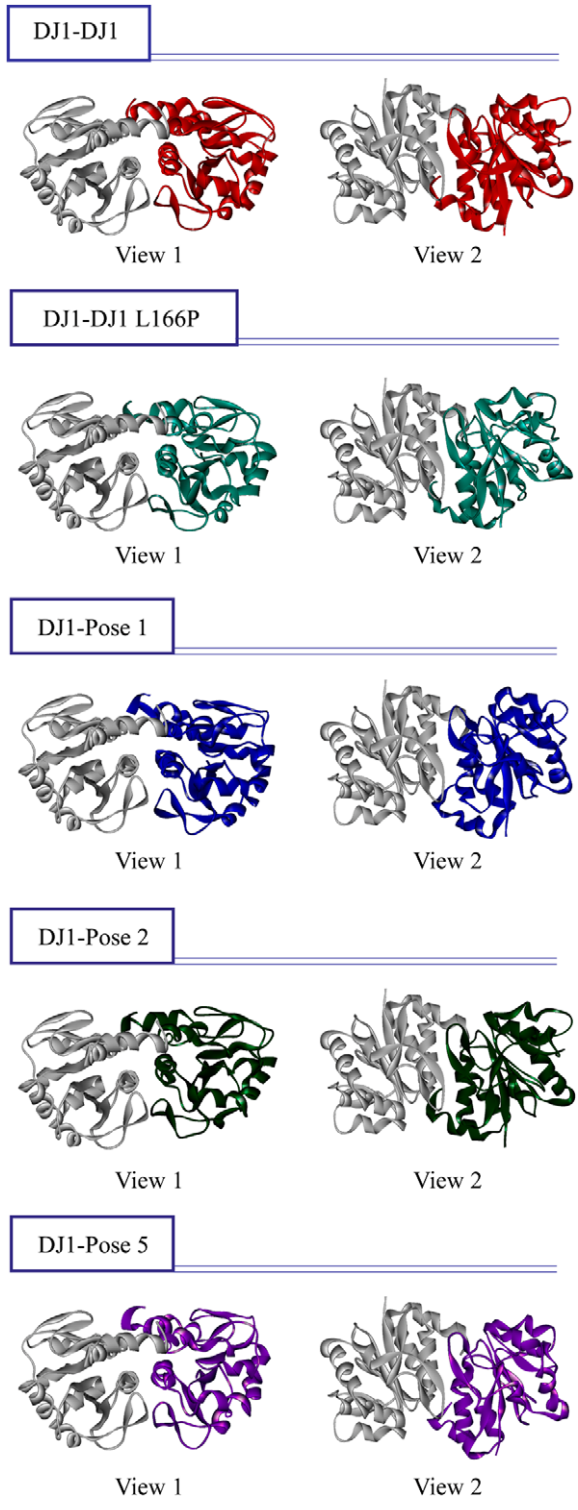

Figure 9. Dimer formation of different DJ1 monomers with wild-type DJ1 monomer by ZDock. DJ1 subunits assessed for dimerization ability include DJ1 (wild type, red), L166P (cyan), Pose 1 (blue), Pose 2 (green), and Pose 5 (purple). The crystal structure of DJ1 is shown in gray. No dimer formation could be detected for Pose 3 and Pose 4.

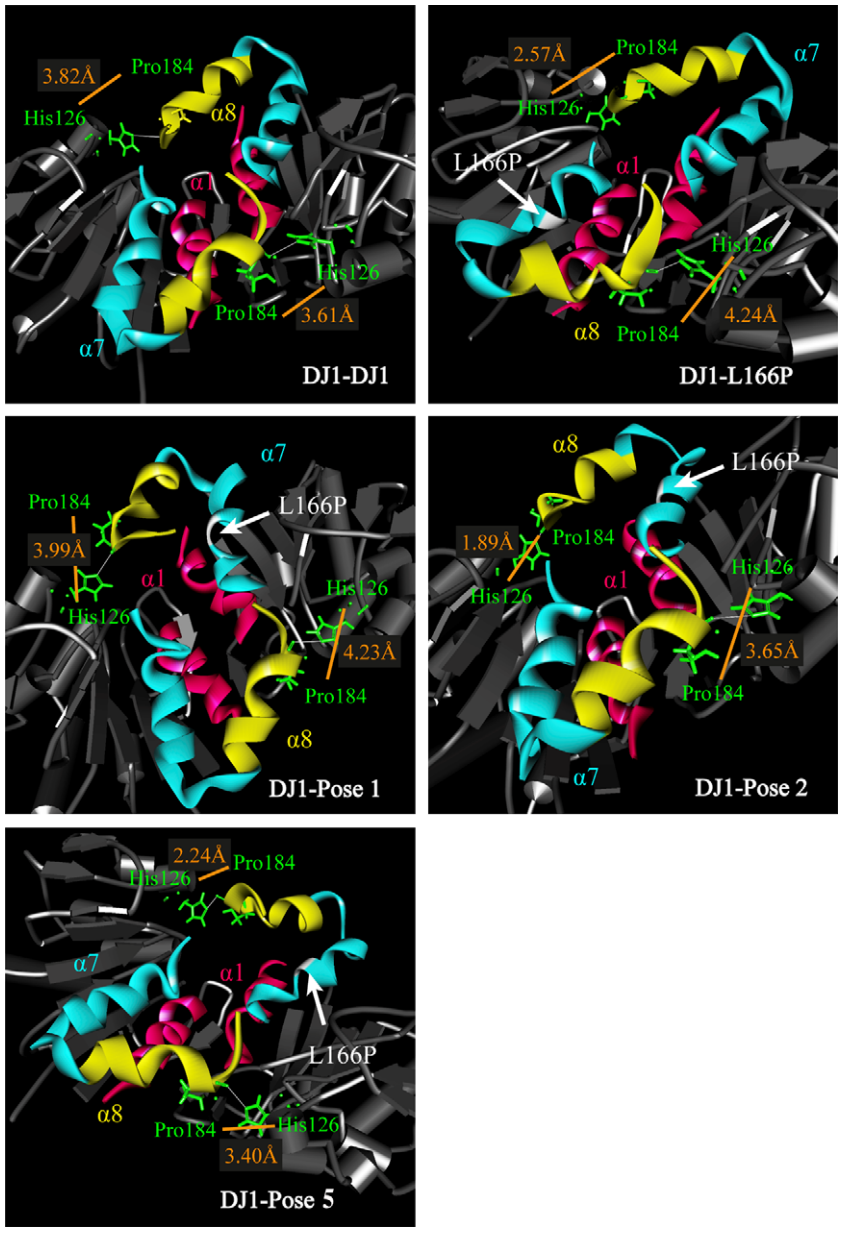

Figure 10. Helix conformations at dimer interface. Helix structures involved in dimer formation include α1 (pink, residues 15–30), α7 (cyan, residues 158–176), and α8 (yellow, residues 177–184). Critical H-bond stabilizing the α-helices for dimer formation is formed between His126 and Pro184 of opposite monomers.

5, dimer RMSDs compared to the crystal DJ1 dimer structure (PDB:2R1T) provide more dynamic insights to the structural integrity of the dimers. As expected, the crystal DJ1 dimer structure and the redocked structure of normal DJ1 after MD simulation were highly similar with a low RMSD of 0.63 Å (Figure 11(b)). The Pose 2-DJ1 dimer also attained high structural similarity to the reference dimer, with RMSDs as low as 0.74 Å (Figure 11(c)). By comparison, Pose 5-DJ1 dimer was structurally deviant from the crystal structure as indicated by the high RMSD values of 3.18 Å (Figure 11(d)).

Conclusion

In this study, we demonstrate possible molecular mechanisms underlying the restore-of-function in L166P by DJ1. By introducing a dock-based dimerization simulation, we identified a BAG1–DJ1 binding pose that may lead to proper dimerization between normal and mutant DJ1s. Interaction between mutant DJ1 and BAG1 at Pose 2 led to restoration of important helix structures in DJ1 monomers and the ability to form dimers with wild-type DJ1. RMSD comparisons indicated that Pose 2-DJ1 dimer was extremely similar to that of the crystal DJ1

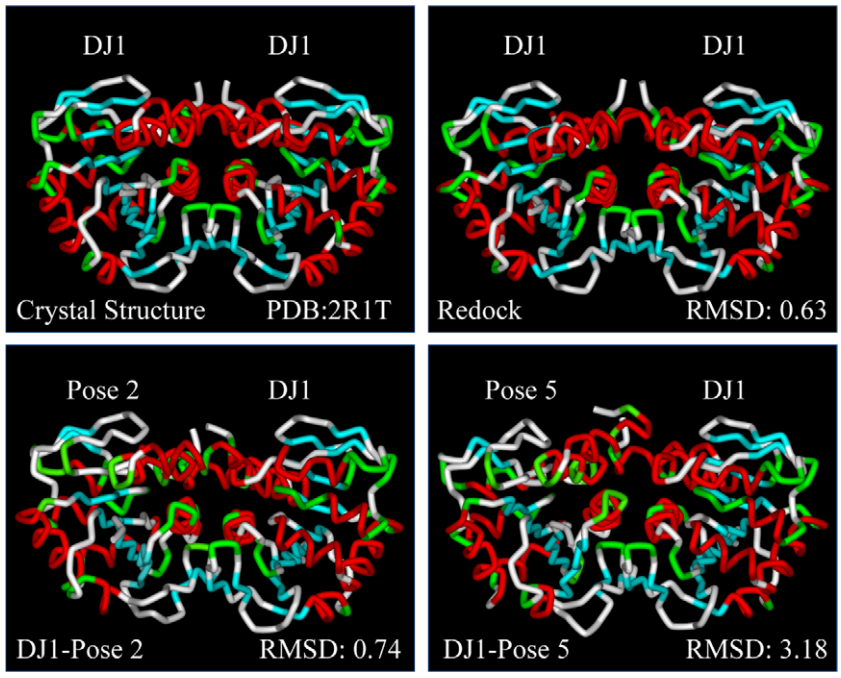

Figure 11. Comparison of DJ1 dimer structures using DJ1 dimer crystal structure (PDB: 2R1T) as the standard. Dimer structures shown are (a) crystal structure of DJ1 dimer, (b) DJ1–DJ1, (c) DJ1-Pose 2, and (d) DJ1-Pose5. Structural similarities are depicted by the measured RMSD. Structures with higher similarity to the crystal structure have smaller RMSD values.

dimer structure. These key findings and relevant Supporting data are summarized in Video 1. Our results provide molecular level explanations on the restoration function of BAG1 on L166P observed in animal models. The information within this study may provide insights into the molecular functions of BAG1, and can be applied to further the search for an effective PD treatment.

Acknowledgments

The research was supported by grants from the National Science Council of Taiwan (NSC 100–2325-B-039–001), Committee on Chinese Medicine and Pharmacy (CCMP100-RD-030), China Medical University and Asia University (DMR-101–094). This study is also supported in part by Taiwan Department of Health Clinical Trial and Research Center of Excellence (DOH101-TD-B-111–004) and Taiwan Department of Health Cancer Research Center of Excellence (DOH101-TD-C-111–005). I thank to the Asia University cloud-computing facilities.

Supplementary material

The supplementary material for this paper is available online at http://dx.doi.org/10.1080/07391102.2012.674182.

References

Anderson, P.C., & Daggett, V. (2008). Molecular basis for the structural instability of human DJ-1 induced by the L166P mutation associated with Parkinson's disease. *Biochemistry, 47*, 9380–9393.

Ariga, H., Kitamura, Y., Watanabe, S., Taguchi, M., Takagi, K., Kawata, T., … Iguchi-Ariga, S.M.M. (2011). Neuroprotective effect of a new DJ-1-binding compound against neurodegeneration in Parkinson's disease and stroke model rats. *Molecular Neurodegeneration, 6*, 48.

Ariga, H., Takahashi-Niki, K., Niki, T., Taira, T., & Iguchi-Ariga, S.M.M. (2004). Reduced anti-oxidative stress activities of DJ-1 mutants found in Parkinson's disease patients. *Biochemical and Biophysical Research Communications, 320*, 389–397.

Batelli, S., Albani, D., Rametta, R., Polito, L., Prato, F., Pesaresi, M., … Forloni, G. (2008). DJ-1 Modulates alpha-Synuclein Aggregation State in a Cellular Model of Oxidative Stress: Relevance for Parkinson's Disease and Involvement of HSP70. *PLoS ONE, 3*, e1884.

Bekris, L.M., Mata, I.F., & Zabetian, C.P. (2010). The genetics of Parkinson disease. *Journal of Geriatric Psychiatry and Neurology, 23*, 228–242.

Bonifati, V., Rizzu, P., van Baren, M.J., Schaap, O., Breedveld, G.J., Krieger, E., … Heutink, P. (2003). Mutations in the DJ-1 gene associated with autosomal recessive early-onset parkinsonism. *Science, 299*, 256–259.

Brooks, B.R., Brooks, C.L., Mackerell, A.D., Nilsson, L., Petrella, R.J., Roux, B., … Karplus, M. (2009). CHARMM: The Biomolecular Simulation Program. *Journal of Computational Chemistry, 30*, 1545–1614.

Cai, Y., He, J., & Lu, L. (2011). Predicting sumoylation site by feature selection method. *Journal of Biomolecular Structure & Dynamics, 28*, 797–804.

Chang, T.T., Chen, K.C., Chang, K.W., Chen, H.Y., Tsai, F.J., Sun, M.F., & Chen, C.Y.C. (2011). In silico pharmacology suggests ginger extracts may reduce stroke risks. *Molecular BioSystems, 7*, 2702–2710.

Chang, S.S., Huang, H.J., & Chen, C.Y.C. (2011a). Two Birds with One Stone? Possible Dual-Targeting H1N1 Inhibitors from Traditional Chinese Medicine. *PLoS Computational Biology, 7*, e1002315.

Chang, S.S., Huang, H.J., & Chen, C.Y.C. (2011b). High performance screening, structural and molecular dynamics analysis to identify H1 inhibitors from TCM Database@Taiwan. *Molecular BioSystems, 7*, 3366–3374.

Chang, T.T., Huang, H.J., Lee, K.J., Yu, H.W., Chen, H.Y., Tsai, F.J., … Chen, C.Y.C. (2010). Key features for designing phosphodiesterase-5 inhibitors. *Journal of Biomolecular Structure & Dynamics, 28*, 309–321.

Chang, T.T., Sun, M.F., Chen, H.Y., Tsai, F.J., Fisher, M., Lin, J.G., & Chen, C.Y.C. (2011). Screening from the world's largest TCM database against H1N1 virus. *Journal of Biomolecular Structure & Dynamics, 28*, 773–786.

Chang, K.W., Tsai, T.Y., Chen, K.C., Yang, S.C., Huang, H.J., Chang, T.T., … Chen, C.Y.C. (2011). ISMART: An integrated cloud computing web server for traditional Chinese medicine for online virtual screening, de novo evolution and drug design. *Journal of Biomolecular Structure & Dynamics, 29*, 243–250.

Chang, P.C., Wang, J.D., Lee, M.M., Chang, S.S., Tsai, T.Y., Chang, K.W., … Chen, C.Y.C. (2011). Lose weight with traditional chinese medicine? Potential suppression of fat mass and obesity-associated protein. *Journal of Biomolecular Structure & Dynamics, 29*, 471–483.

Checkoway, H., & Nelson, L.M. (1999). Epidemiologic approaches to the study of Parkinson's disease etiology. *Epidemiology, 10*, 327–336.

Chen, C.Y.C. (2010). Virtual screening and drug design for PDE-5 Receptor from traditional Chinese medicine database. *Journal of Biomolecular Structure & Dynamics, 27*, 627–640.

Chen, C.Y.C. (2011). TCM Database@Taiwan: The world's largest traditional Chinese medicine database for drug screening in silico. *PLoS ONE, 6*, e15939.

Chen, K.C., Chang, K.W., Chen, H.Y., & Chen, C.Y.C. (2011). Traditional Chinese medicine, a solution for reducing dual stroke risk factors at once? *Molecular BioSystems, 7*, 2711–2719.

Chen, C.Y., & Chen, C.Y.C. (2010). Insights into designing the dual-targeted HER2/HSP90 inhibitors. *Journal of Molecular Graphics and Modelling, 29*, 21–31.

Chen, K.C., & Chen, C.Y.C. (2011). Stroke prevention by traditional Chinese medicine? A genetic algorithm, support vector machine and molecular dynamics approach. *Soft Matter, 7*, 4001–4008.

Chen, R., Li, L., & Weng, Z. (2003). ZDOCK: An initial-stage protein-docking algorithm. *Proteins, 52*, 80–87.

Chen, K.C., Sun, M.F., Yang, S.C., Chang, S.S., Chen, H.Y., Tsai, F.J., & Chen, C.Y.C. (2011). Investigation into Potent Inflammation Inhibitors from Traditional Chinese Medicine. *Chemical Biology & Drug Design, 78*, 679–688.

Chen, R., & Weng, Z. (2003). A novel shape complementarity scoring function for protein-protein docking. *Proteins, 51*, 397–408.

de Rijk, M.C., Launer, L.J., Berger, K., Breteler, M.M., Dartigues, J.F., Baldereschi, M., … Hofman, A. (2000). Prevalence of Parkinson's disease in Europe: A collaborative study of population-based cohorts. Neurologic Diseases in the Elderly Research Group. *Neurology, 54*, S21–23.

Deeg, S., Gralle, M., Sroka, K., Bahr, M., Wouters, F.S., & Kermer, P. (2010). BAG1 restores formation of functional DJ-1 L166P dimers and DJ-1 chaperone activity. *Journal of Cell Biology, 188*, 505–513.

Friedman, J.S., Xu, X.L., & Martin, F. (2010). The familial Parkinson's disease gene DJ-1 (PARK7) is expressed in red cells and plays a role in protection against oxidative damage. *Blood Cells Molecules and Diseases, 45*, 227–232.

Guimaraes, A.P., Oliveira, A.A., da Cunha, E.F.F., Ramalho, T. C., & Franca, T.C.C. (2011). Design of New Chemotherapeutics Against the Deadly Anthrax Disease. Docking and Molecular Dynamics Studies of Inhibitors Containing Pyrrolidine and Riboamidrazone Rings on Nucleoside Hydrolase from Bacillus anthracis. *Journal of Biomolecular Structure & Dynamics, 28*, 455–469.

Hague, A., Wood, J., Pring, M., Eveson, J.W., Price, N., & Proby, C.M. (2011). Co-overexpression of Bag-1 and heat shock protein 70 in human epidermal squamous cell carcinoma: Bag-1-mediated resistance to 5-fluorouracil-induced apoptosis. *British Journal of Cancer, 104*, 1459–1471.

Heisters, D. (2011). Parkinson's: Symptoms, treatments and research. *British Journal of Nursing, 20*, 548–554.

Hering, R., Strauss, K.M., Tao, X., Bauer, A., Woitalla, D., Mietz, E.M., … Riess, O. (2004). Novel homozygous p. E64D mutation in DJ1 in early onset Parkinson disease (PARK7). *Human Mutation, 24*, 321–329.

Honbou, K., Suzuki, N.N., Horiuchi, M., Niki, T., Taira, T., Ariga, H., & Inagaki, F. (2003). The crystal structure of DJ-1, a protein related to male fertility and Parkinson's disease. *Journal of Biological Chemistry, 278*, 31380–31384.

Huai, Q., Sun, Y., Wang, H., Chin, L.S., Li, L., Robinson, H., & Ke, H. (2003). Crystal structure of DJ-1/RS and implication on familial Parkinson's disease. *FEBS Letters, 549*, 171–175.

Huang, H.J., Lee, K.J., Yu, H.W., Chen, C.Y., Hsu, C.H., Chen, H.Y., … Chen, C.Y.C. (2010). Structure-Based and Ligand-Based Drug Design for HER 2 Receptor. *Journal of Biomolecular Structure & Dynamics, 28*, 23–37.

Huang, H.J., Lee, K.J., Yu, H.W., Chen, H.Y., Tsai, F.J., & Chen, C.Y.C. (2010). A novel strategy for designing the selective PPAR agonist by the "sum of activity" model. *Journal of Biomolecular Structure & Dynamics, 28*, 187–200.

Huang, H.J., Yu, H.W., Chen, C.Y., Hsu, C.H., Chen, H.Y., Lee, K.J., … Chen, C.Y.C. (2010). Current developments of computer-aided drug design. *Journal of the Taiwan Institute of Chemical Engineers, 41*, 623–635.

Hung, W.J., Roberson, R.S., Taft, J., & Wu, D.Y. (2003). Human BAG-1 proteins bind to the cellular stress response protein GADD34 and interfere with GADD34 functions. *Molecular and Cellular Biology, 23*, 3477–3486.

Irrcher, I., Aleyasin, H., Seifert, E.L., Hewitt, S.J., Chhabra, S., Phillips, M., … Park, D.S. (2010). Loss of the Parkinson's disease-linked gene DJ-1 perturbs mitochondrial dynamics. *Human Molecular Genetics, 19*, 3734–3746.

Ishikawa, S., Taira, T., Takahashi-Niki, K., Niki, T., Ariga, H., & Iguchi-Ariga, S.M. (2010). Human DJ-1-specific transcriptional activation of tyrosine hydroxylase gene. *Journal of Biological Chemistry, 285*, 39718–39731.

Kahle, P.J., Waak, J., & Gasser, T. (2009). DJ-1 and prevention of oxidative stress in Parkinson's disease and other age-related disorders. *Free Radical Biology and Medicine, 47*, 1354–1361.

Kermer, P., Digicaylioglu, M.H., Kaul, M., Zapata, J.M., Krajewska, M., Stenner-Liewen, F., … Reed, J.C. (2003). BAG1 over-expression in brain protects against stroke. *Brain Pathology, 13*, 495–506.

Kermer, P., Sroka, K., Voigt, A., Deeg, S., Reed, J.C., Schulz, J.B., & Bahr, M. (2009). BAG1 modulates huntingtin toxicity, aggregation, degradation, and subcellular distribution. *Journal of Neurochemistry, 111*, 801–807.

Lin, C.H., Chang, T.T., Sun, M.F., Chen, H.Y., Tsai, F.J., Chang, K.L., … Chen, C.Y.C. (2011). Potent Inhibitor Design Against H1N1 Swine Influenza: Structure-based and Molecular Dynamics Analysis for M2 Inhibitors from Traditional Chinese Medicine Database. *Journal of Biomolecular Structure & Dynamics, 28*, 471–482.

Macedo, M.G., Anar, B., Bronner, I.F., Cannella, M., Squitieri, F., Bonifati, V., … Rizzu, P. (2003). The DJ-1L166P mutant protein associated with early onset Parkinson's disease is unstable and forms higher-order protein complexes. *Human Molecular Genetics, 12*, 2807–2816.

Mak, T.W., Aleyasin, H., Rousseaux, M.W.C., Phillips, M., Kim, R.H., Bland, R.J., … Park, D.S. (2007). The Parkinson's disease gene DJ-1 is also a key regulator of stroke-induced damage. *Proceedings of the National academy of Sciences of the United States of America, 104*, 18748–18753.

Mei, Z., Liu, J., & Yu, H. (2011). Modeling of transition state by molecular dynamics. Prediction of catalytic efficiency of the mutants of mandelate racemase. *Journal of Biomolecular Structure & Dynamics, 28*, 871–879.

Miller, D.W., Ahmad, R., Hague, S., Baptista, M.J., Canet-Aviles, R., McLendon, C., … Cookson, M.R. (2003). L166P mutant DJ-1, causative for recessive Parkinson's disease, is degraded through the ubiquitin-proteasome system. *Journal of Biological Chemistry, 278*, 36588–36595.

Moore, D.J., Zhang, L., Dawson, T.M., & Dawson, V.L. (2003). A missense mutation (L166P) in DJ-1, linked to familial Parkinson's disease, confers reduced protein stability and impairs homo-oligomerization. *Journal of Neurochemistry, 87*, 1558–1567.

Nuytemans, K., Theuns, J., Cruts, M., & Van Broeckhoven, C. (2010). Genetic etiology of Parkinson disease associated with mutations in the SNCA, PARK2, PINK1, PARK7, and LRRK2 genes: A mutation update. *Human Mutation, 31*, 763–780.

Rochet, J.C., Liu, F., Nguyen, J.L., Hulleman, J.D., & Li, L. (2008). Mechanisms of DJ-1 neuroprotection in a cellular model of Parkinson's disease. *Journal of Neurochemistry, 105*, 2435–2453.

Roy, A., Kucukural, A., & Zhang, Y. (2010). I-TASSER: A unified platform for automated protein structure and function prediction. *Nature Protocols, 5*, 725–738.

Sanderson, K. (2011). Databases aim to bridge the East-West divide of drug discovery. *Nature Medicine, 17*, 1531.

Semighini, E.P., Resende, J.A., de Andrade, P., Morais, P.A., Carvalho, I., Taft, C.A., & Silva, C.H. (2011). Bag1 is essential for differentiation and survival of hematopoietic and neuronal cells. *Journal of Biomolecular Structure & Dynamics, 28*, 787–796.

Sendtner, M., Gotz, R., Wiese, S., Takayama, S., Camarero, G. C., … Rapp, U.R. (2005). Bag1 is essential for differentiation and survival of hematopoietic and neuronal cells. *Nature Neuroscience, 8*, 1169–1178.

Sondermann, H., Scheufler, C., Schneider, C., Hohfeld, J., Hartl, F.U., & Moarefi, I. (2001). Structure of a Bag/Hsc70 complex: Convergent functional evolution of Hsp70 nucleotide exchange factors. *Science, 291*, 1553–1557.

Sun, M.F., Chang, T.T., Chang, K.W., Huang, H.J., Chen, H.Y., Tsai, F.J., … Chen, C.Y.C. (2011). Blocking the DNA repair system by traditional Chinese medicine? *Journal of Biomolecular Structure & Dynamics, 28*, 895–906.

Sun, M.F., Chen, H.Y., Tsai, F.J., Lui, S.H., & Chen, C.Y.C. (2011). Search for novel remedies to augment radiation resistance of inhabitants of Fukushima and Chernobyl disasters: Identifying DNA repair protein XRCC4 inhibitors. *Journal of Biomolecular Structure & Dynamics, 29*, 325–337.

Surmeier, D.J., Guzman, J.N., Sanchez-Padilla, J., Wokosin, D., Kondapalli, J., Ilijic, E., & Schumacker, P.T. (2010). Oxidant stress evoked by pacemaking in dopaminergic neurons is attenuated by DJ-1. *Nature, 468*, 696–700.

Taira, T., Saito, Y., Niki, T., Iguchi-Ariga, S.M., Takahashi, K., & Ariga, H. (2004). DJ-1 has a role in antioxidative stress to prevent cell death. *EMBO Reports, 5*, 213–218.

Takayama, S., Bimston, D.N., Matsuzawa, S., Freeman, B.C., Aime-Sempe, C., Xie, Z., … Reed, J.C. (1997). BAG-1 modulates the chaperone activity of Hsp70/Hsc70. *EMBO Journal, 16*, 4887–4896.

Tao, X., & Tong, L. (2003). Crystal structure of human DJ-1, a protein associated with early onset Parkinson's disease. *Journal of Biological Chemistry, 278*, 31372–31379.

Tarantino, P., Annesi, F., Scornaienchi, V., Rocca, F.E., De Marco, E.V., Civitelli, D., … Annesi, G. (2010). Novel human pathological mutations. Gene symbol: PARK7. Disease: Parkinson disease. *Human Genetics, 127*, 463.

Ting, J.P.Y., Mcnally, R.S., Davis, B.K., Clements, C.M., Accavitti-Loper, M.A., & Mak, T.W. (2011). DJ-1 enhances cell survival through the binding of Cezanne, a negative regulator of NF-kappa B. *Journal of Biological Chemistry, 286*, 4098–4106.

Townsend, P.A., Stephanou, A., Packham, G., & Latchman, D. S. (2005). BAG-1: A multi-functional pro-survival molecule. *International Journal of Biochemistry and Cell Biology, 37*, 251–259.

Tsai, T.Y., Chang, K.W., & Chen, C.Y.C. (2011). IScreen: World's first cloud-computing web server for virtual screening and de novo drug design based on TCM database@Taiwan. *Journal of Computer-Aided Molecular Design, 25*, 525–531.

Waragai, M., Nakai, M., Wei, J., Fujita, M., Mizuno, H., Ho, G., … Hashimoto, M. (2007). Plasma levels of DJ-1 as a possible marker for progression of sporadic Parkinson's disease. *Neuroscience Letters, 425*, 18–22.

Williams, A.C., Barnes, J.D., Arhel, N.J., Lee, S.S., Sharp, A., Al-Okail, M., … Paraskeva, C. (2005). Nuclear BAG-1 expression inhibits apoptosis in colorectal adenoma-derived epithelial cells. *Apoptosis, 10*, 301–311.

Wilson, M.A., Collins, J.L., Hod, Y., Ringe, D., & Petsko, G.A. (2003). The 1.1-A resolution crystal structure of DJ-1, the protein mutated in autosomal recessive early onset Parkinson's disease. *Proceedings of the National academy of Sciences of the United States of America, 100*, 9256–9261.

Wirdefeldt, K., Adami, H.O., Cole, P., Trichopoulos, D., & Mandel, J. (2011). Epidemiology and etiology of Parkinson's disease: A review of the evidence. *European Journal of Epidemiology, 26* (Suppl 1), S1–58.

Xiong, H., Wang, D., Chen, L., Choo, Y.S., Ma, H., Tang, C., … Zhang, Z. (2009). Parkin, PINK1, and DJ-1 form a ubiquitin E3 ligase complex promoting unfolded protein degradation. *The Journal of Clinical Investigation, 119*, 650–660.

Yang, S.C., Chang, S.S., & Chen, C.Y.C. (2011). Identifying HER2 inhibitors from natural products database. *PLoS ONE, 6*, e28793.

Yang, S.C., Chang, S.S., Chen, H.Y., & Chen, C.Y.C. (2011). Identification of potent EGFR inhibitors from TCM Database@Taiwan. *PLoS Computational Biology, 7*, e1002189.

Zhou, W., Zhu, M., Wilson, M.A., Petsko, G.A., & Fink, A.L. (2006). The oxidation state of DJ-1 regulates its chaperone activity toward alpha-synuclein. *Journal of Molecular Biology, 356*, 1036–1048.